UCRL-16770

University of California

Ernest O. Lawrence Radiation Laboratory

DISLOCATION MECHANISM IN AN IRON-MANGANESE ALLOY AT LOW TEMPERATURES

TWO-WEEK LOAN COPY

This is a Library Circulating Copy which may be borrowed for two weeks. For a personal retention copy, call Tech. Info. Division, Ext. 5545

DISCLAIMER

This document was prepared as an account of work sponsored by the United States Government. While this document is believed to contain correct information, neither the United States Government nor any agency thereof, nor the Regents of the University of California, nor any of their employees, makes any warranty, express or implied, or assumes any legal responsibility for the accuracy, completeness, or usefulness of any information, apparatus, product, or process disclosed, or represents that its use would not infringe privately owned rights. Reference herein to any specific commercial product, process, or service by its trade name, trademark, manufacturer, or otherwise, does not necessarily constitute or imply its endorsement, recommendation, or favoring by the United States Government or any agency thereof, or the Regents of the University of California. The views and opinions of authors expressed herein do not necessarily state or reflect those of the United States Government or any agency thereof or the Regents of the University of California.

UCRL-16770

UNIVERSITY OF CALIFORNIA
Lawrence Radiation Laboratory
Berkeley, California

AEC Contract No. W-7405-eng-48

DISLOCATION MECHANISMS IN AN IRON-MANGANESE ALLOY AT LOW TEMPERATURES

Paul Pinhas Wynblatt

(Ph.D. Thesis)

June, 1966

CONTENTS

ABSTRACT

I. INTRODUCTION 1

II. EXPERIMENTAL PROCEDURE AND RESULTS 2

III. DISCUSSION 5

IV. CONCLUSIONS 20

V. ACKNOWLEDGMENTS 20

REFERENCES 21

DISLOCATION MECHANISMS IN AN IRON-MANGANESE ALLOY AT LOW TEMPERATURES

Paul Pinhas Wynblatt

Inorganic Materials Research Division, Lawrence Radiation Laboratory
Department of Mineral Technology, College of Engineering
University of California, Berkeley, California

ABSTRACT

June 1966

The effect of strain rate, temperature and interstitial impurity concentration on the flow stress was investigated in a polycrystalline iron-2% manganese alloy. The temperature dependence of the flow stress was found to be independent of the interstitial impurity concentration, removal of interstitials merely decreasing the athermal stress level. Below 160°K, the large temperature dependence of the flow stress was interpreted in terms of the Dorn-Rajnak theory of the Peierls mechanism of plastic deformation. Above 160°K, some other thermally activated intrinsic mechanism seems to be operating.

I. INTRODUCTION

The strong temperature dependence of the flow stress of b.c.c. iron at low temperatures has been studied by numerous investigators and interpreted in terms of several different thermally activated dislocation mechanisms. The following mechanisms have been proposed:

(a) Interaction of dislocations with interstitial impurity atoms[1] or with solute atoms in general,[2]

(b) Intersection of dislocations with clusters of impurity atoms,[3]

(c) Resistance to the motion of dislocations due to jogs on screw dislocations,[4]

(d) Resistance to the motion of dislocations due to the Snoeck effect[5] and,

(e) Interaction of dislocations with the intrinsic resistance of the b.c.c. lattice or Peierls' "hills".[6-8]

In previous work,[9] it was found that the plastic behavior of polycrystalline iron containing 2 wt.% Mn (and 100 p.p.m. carbon + nitrogen) is in good agreement with predictions based on the Peierls' mechanism[10] from 77°K to 160°K whereas from 160°K to about 370°K another as yet unidentified thermally activated mechanism is operative.

The purpose of the present investigation was to determine the effect of interstitial impurities on the temperature dependence of the flow stress, by purifying the previously investigated alloy with respect to interstitial impurities. The investigation revealed that removal of the interstitial impurities to a level that eliminated Cottrell locking and the Portevin-LeChatelier effect affects neither the strong temperature dependence of the flow stress at low temperatures nor the

general characteristics of the higher temperature behavior. Such purification, however, lowered the athermal yield stress.

II. EXPERIMENTAL PROCEDURE AND RESULTS

The material used in this investigation consisted of an iron 2 wt.% manganese alloy having the following additional elements present: 0.004% C, 0.006% N, 0.05% O, 0.004% P and 0.001% Si. This was the same material as that studied in the previous investigation and will henceforth be referred to as the "impure material". The as received 3/8" x 3/4" hot rolled bars were cold rolled to 0.08" thickness, recrystallized under argon for 30 minutes at 800°C and further cold rolled to 0.053" thickness. Flat tensile specimens 1/4" wide having a 1.625" long gage section were machined from the sheet and then purified.

The first stage of purification consisted of holding the specimens at 850°C for 24 hours in a stream of hydrogen saturated with water vapor at room temperature. Material prepared in this fashion will subsequently be referred to as "wet hydrogen purified material". It has been estimated that this type of treatment reduces the carbon content of iron to less than 5 p.p.m.[1]

The second stage of purification consisted of holding the specimens in a closed system through which hydrogen was circulated past the heated specimens as well as a zirconium hydride getter. The specimens were held at 850°C and the getter at 800°C. The process was continued for 212 hours. The starting material for this process was wet hydrogen

purified material. Material prepared in this manner will be referred to as "ZrH_2 purified material". The technique used was substantially the same as that described by Stein et al.[1] who have shown that the carbon level at the end of the process is reduced to about 5 parts per billion.

All tensile testing was carried out on an Instron Testing Machine either in controlled temperature baths or at fixed point baths such as boiling liquid nitrogen, etc... When fixed points were used the temperature was kept constant to better than ±1°C whereas in all other tests the temperature variation was less than ±2°C.

Test of Purity

It was not possible to determine the purity achieved at each stage of the purification because the resulting level of interstitial impurities was well below the limit of sensitivity of standard analytical techniques. It was possible, however, to obtain a qualitative measure of the extent of purification from the appearance of the stress strain curves for the three materials. Figure 1 shows the stress strain curves for the three different materials tested at 300°K. It can be seen that the effect of wet hydrogen purification on the impure material was threefold. The upper yield point was entirely eliminated, the lower yield stress was decreased and the extent of Lüders band strain was reduced by about a factor of ten. The three effects provide strong evidence that a significant reduction of the interstitial content was achieved. The effect of ZrH_2 purification was to eliminate all yield and Lüders band phenomena. These trends are in substantial

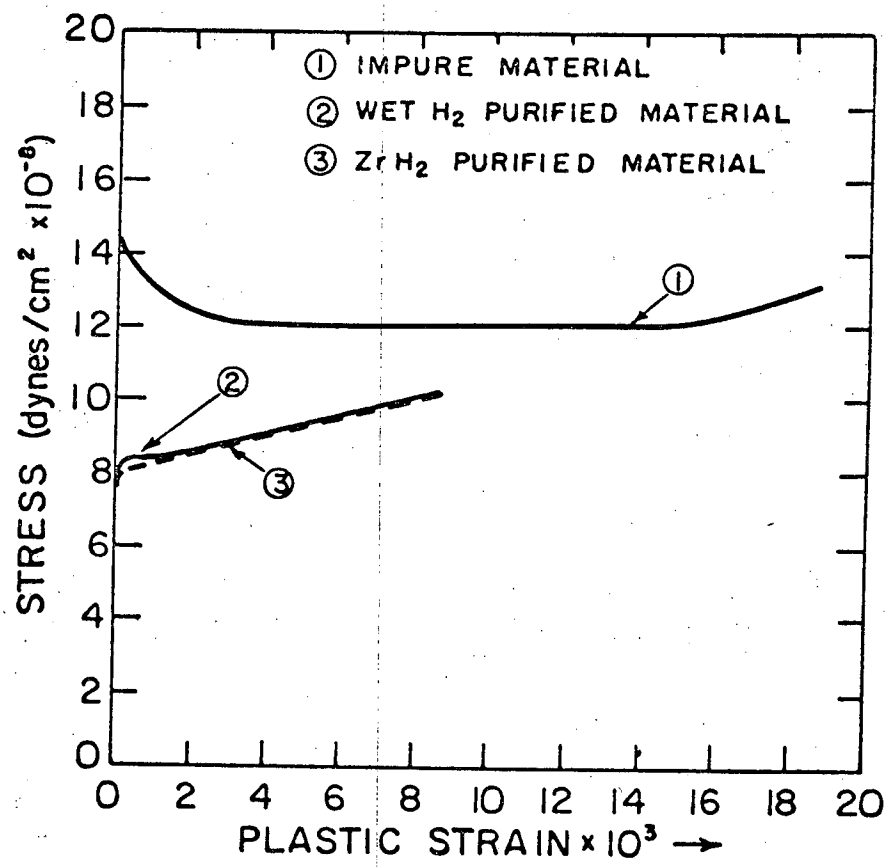

Figure 1. Stress-strain curves at 300°K on original specimens.

MU-37205

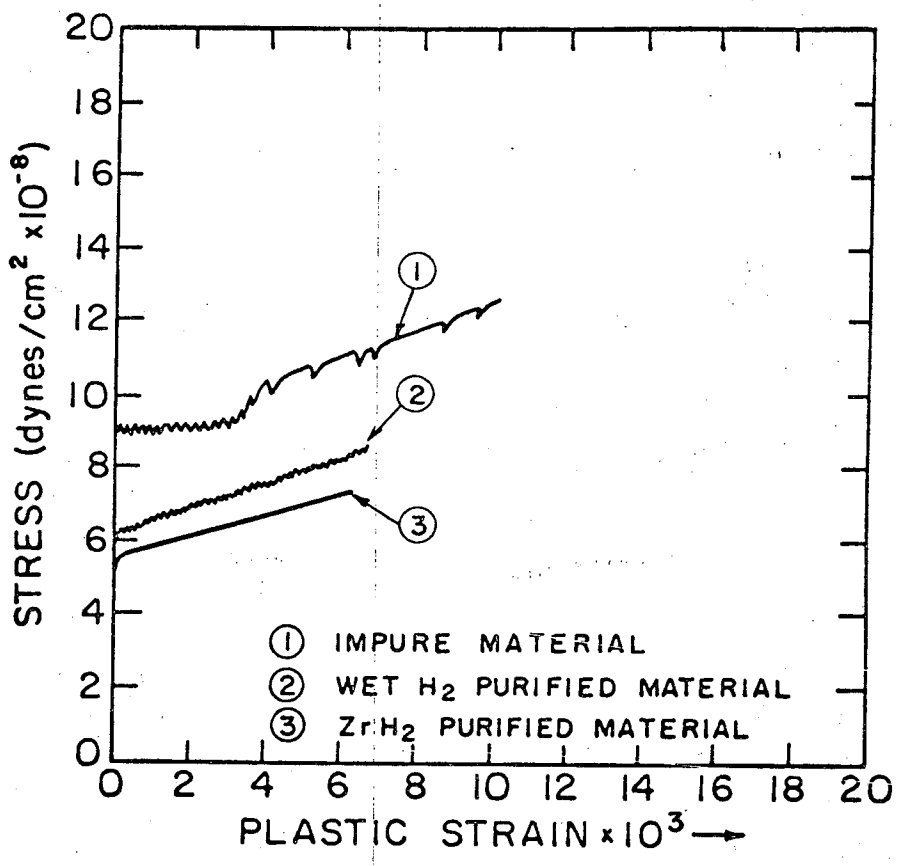

Figure 2. Stress-strain curves at 523°K on original specimens.

MU-37206

agreement with those obtained by Stein et al.[1]

Figure 2 shows the stress-strain curves for the three materials tested at 523°K. It can be seen that the impure and wet hydrogen purified materials exhibited a marked Portevin-LeChatelier effect indicating that interstitial impurities were still present in the wet hydrogen purified material. In contrast to these results, however, the ZrH_2 purified material exhibited no sign of the Portevin-LeChatelier effect thus indicating that the concentration of interstitial impurities was so low as to make dislocation-impurity interactions undetectable.

Experimental Results

For convenience in the theoretical analysis, the data are presented in terms of the shear stress for flow, τ, the shear strain γ and the shear strain rate $\dot{\gamma}$. Tensile specimens of the wet hydrogen and ZrH_2 purified materials were prestrained at 423°K at a shear strain rate of 1.54×10^{-5}/sec to stress levels of 3.64×10^8 and 3.21×10^8 dynes/cm^2 respectively. Immediately following this prestrain the temperature bath was changed and each specimen tested in tension at either $\dot{\gamma} = 1.54 \times 10^{-5}$/sec or 1.54×10^{-3}/sec. The values obtained for the stress were within ±2% of the stated shear stress and ±5% of the reported values of the strain rate. The tensile stresses were converted to shear stresses using a factor of 1/2 and the shear strains obtained from engineering strains using a factor of 3/2. The shear stress for the initiation of flow at the test temperature was determined by taking a $\gamma = 9.24 \times 10^{-3}$ offset from the modulus line at which good accuracy was achieved in determining $\dot{\gamma}$ and the associated flow stress τ.

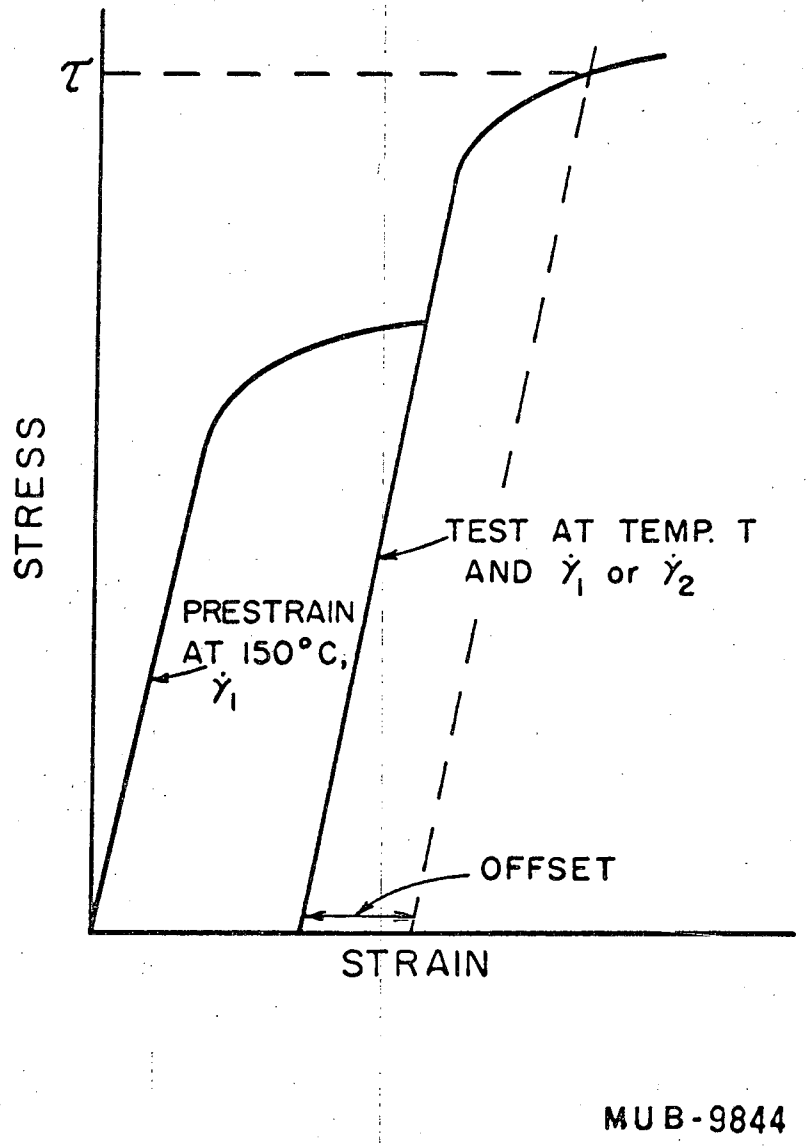

MUB-9844

Figure 3. Diagramatic representation of testing procedure.

A schematic representation of the testing procedure is given in Fig. 3. Typical experimental stress-strain curves for the wet hydrogen and ZrH_2 purified materials are shown in Figs. 4a and 4b respectively.

The experimentally determined flow stresses for the wet hydrogen and ZrH_2 purified materials are plotted against temperature in Fig. 5. Similar data for the impure material, as determined earlier,[9] are given in Fig. 6 for comparison.

The microstructures of the wet hydrogen and ZrH_2 purified materials were not noticeably different. However, both of these materials showed a grain size that was about 5 times larger than that of the impure material. In order to evaluate the effect of grain size on the measured flow stresses, some wet hydrogen purified material was grain-refined to produce a grain size similar to that of the impure material. Although the different grained samples had significantly different yield stresses, in accordance with the Petch equation, it was found that after a few percent prestrain the behavior of the two kinds of sample was identical. This effect is presumably due to the formation of cells of fixed size, independent of the original grain size.

The ZrH_2 purified material behaved in a brittle manner at temperatures below about 100°K. Metallographic examination showed that twinning occurred in the immediate vicinity of the fracture.

III. DISCUSSION

Examination of Figs. 5 and 6 shows that the flow stress dependence on the temperature is independent of the concentration of interstitial

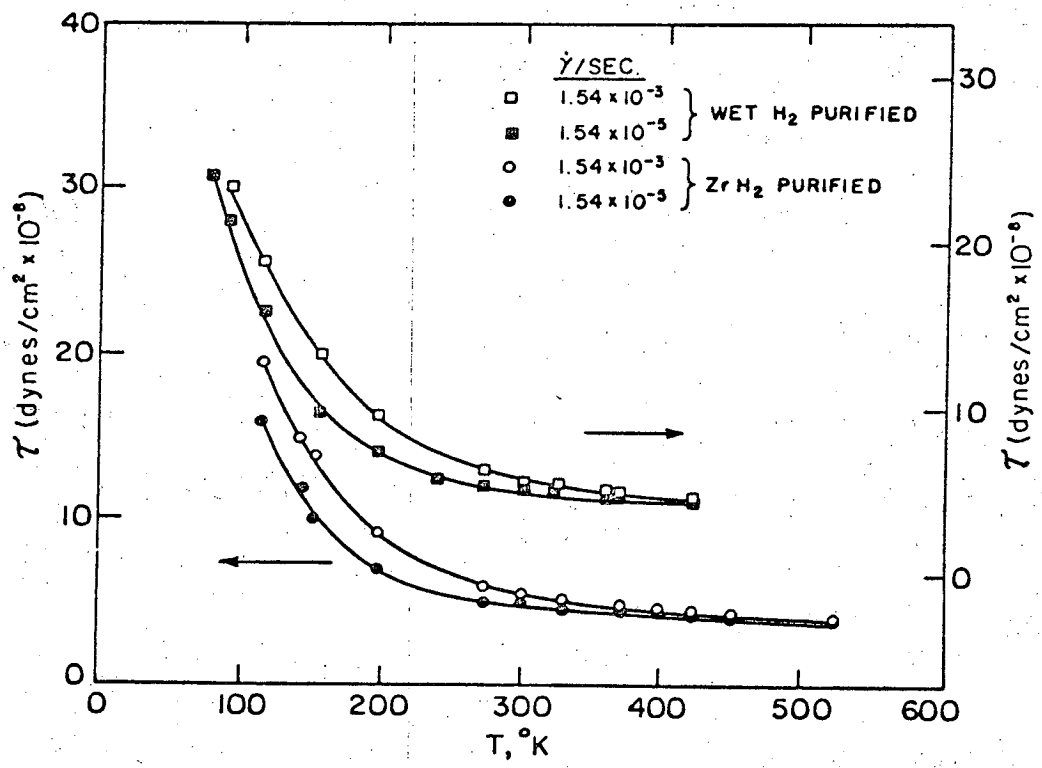

MU-37207

Figure 5. Flow stress vs. temperature curves for the wet hydrogen and ZrH_2 purified materials prestrained to 3.64×10^8 and 3.21×10^8 dynes/cm^2 respectively at 423°K.

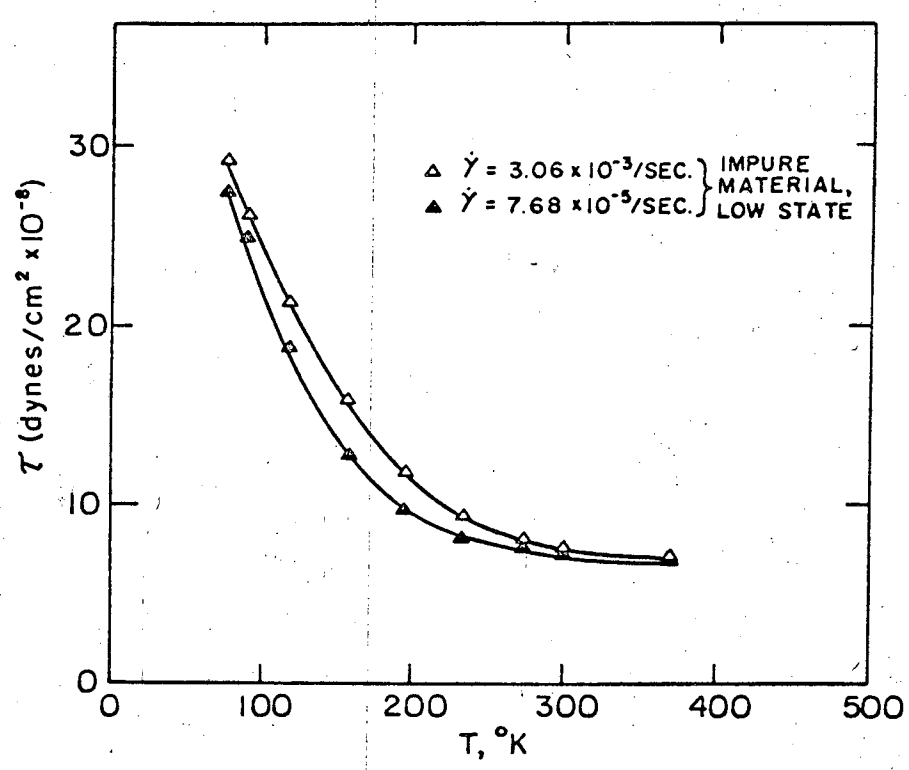

MU-37208

Figure 6. Flow stress vs. temperature curves for the impure material prestrained to 6.89×10^8 dynes/cm^2 at 300°K.

impurities. In earlier work,[9] the impure material was tested in three different strain hardened states and it was established that the temperature dependence of the flow stress did not depend on the strain hardened state. The data from the previous investigation were analyzed in terms of the Dorn-Rajnak[10] model of dislocation motion controlled by nucleation of a pair of kinks over Peierls' barriers and were found to fit the model extremely well in the range 77° to 160°K. In view of the earlier success of that approach and of the observation that the temperature dependence of the flow stress is independent of the concentration of interstitial impurities or of the strain hardened state (i.e. dislocation density), it is reasonable to apply the same analysis to the present data.

The Dorn-Rajnak Model

It was first suggested by Peierls[11] that dislocations tend to lie in potential valleys parallel to close packed rows of atoms. When a dislocation is moved as a whole from the bottom of a potential (or Peierls') valley to the top of a potential hill its line energy is increased from Γ_o to Γ_c because of the straining of bonds in the vicinity of the dislocation core. Thus the magnitude of the line energy of a dislocation is a function of its position, y, and can be written as $\Gamma\{y\}$. In the Dorn-Rajnak model, the shape of the potential hills was assumed to be of the form

$$\Gamma\{y\} = \frac{\Gamma_c + \Gamma_o}{2} + \frac{\Gamma_c - \Gamma_o}{2}\left(\frac{\alpha}{2} + \cos\frac{2\pi y}{a} - \frac{\alpha}{4}\cos\frac{4\pi y}{a}\right) \qquad (1)$$

where a is the distance between parallel rows of close packed atoms and α is a shape factor. For $\alpha = 0$, $\Gamma\{y\}$ becomes a simple cosine function of the displacement, whereas for positive or negative values of α the breadth of the potential hills is made either smaller or larger without changing the periodicity or the maximum and minimum values of the line energy. The stress τ^* that is needed to move the dislocation line to a position y_o, part of the way up the potential hills, is given by

$$\tau^* b = \left(\frac{\partial \Gamma\{y\}}{\partial y}\right)_{y=y_o} = -\frac{\pi}{a}(\Gamma_c - \Gamma_o)\sin\frac{2\pi y_o}{a}\left\{1 - \alpha\cos\frac{2\pi y_o}{a}\right\} \qquad (2)$$

where b is the Burgers vector of the dislocation. The Peierls stress, τ_p, is the stress necessary to move a dislocation over the potential hills in the absence of thermal activation and is obtained by maximizing τ^*,

$$\tau_p b = \frac{\pi}{16a}\frac{(\Gamma_c - \Gamma_o)}{|\alpha|}[3 + (1 + 8\alpha^2)^{1/2}][8\alpha^2 - 2 + 2(1 + 8\alpha^2)^{1/2}]^{1/2} \qquad (3)$$

When a stress $\tau^* < \tau_p$ is applied, the dislocation will move up the Peierls hill to a point y_o as illustrated in Fig. 7. The model assumes that further motion of the dislocation occurs by the thermal nucleation of a double kink over the remaining portion of the barrier as shown in the figure. In order to determine the critical double kink configuration (i.e. the shape of the minimum energy double kink having equal probability of moving forward or collapsing back) an expression for the energy necessary to form a double kink is set up and minimized. The energy to form a double kink can be written

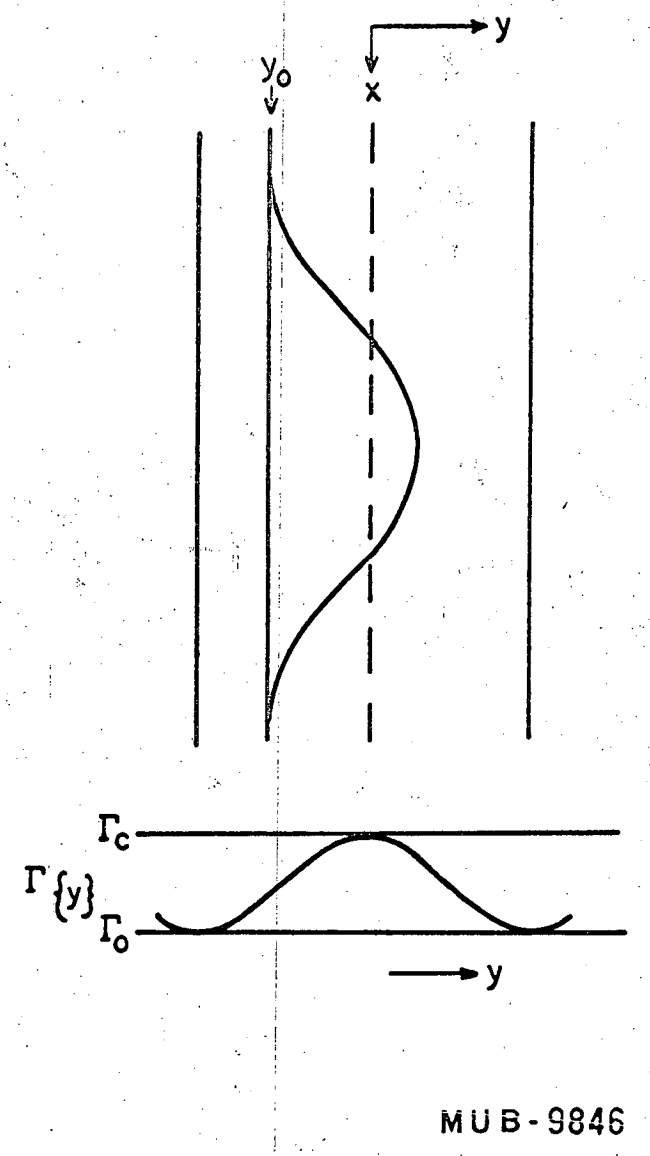

Figure 7. Model for nucleation of a pair of kinks.

$$Un = \int_{-\infty}^{\infty} \Gamma\{y\}ds - \Gamma\{y_o\}dx - \tau^* b(y - y_o)dx \qquad (4)$$

where the first term of the integrand refers to the line energy of the thermally displaced dislocation $y = y\{x\}$, the second term to the original line energy of the dislocation when it was displaced to $y = yo$ under the stress τ^* and the third term to the work done by the stress as the double kink is formed. By using the Euler equation of variational calculus it is possible to determine the shape of the dislocation $y = y\{x\}$ for which the energy is a minimum. The integral, however, could not be solved analytically so that a numerical solution had to be obtained. This numerical solution relates Un and τ^*. The energy of an isolated kink under zero stress, U_k, was obtained by the same variational technique, using this value of the kink energy and the value of τ_p obtained from Eq. (3), the numerical relationship between Un and τ^* was expressed in dimensionless form as

$$\frac{\tau^*}{\tau_p} = f_1 \left(\frac{Un}{2U_k}\right) \qquad (5)$$

where f_1 is not known analytically but is available from the numerical solution of Eq. (4). Eq. (5) is plotted in Fig. 8 for three values of the shape factor α ranging from -1 to + 1. It is interesting to note that the relationship between Un and τ^* is not much affected by the shape of the Peierls hills in the range investigated. The calculated values of τ_p and U_k can be compared as follows

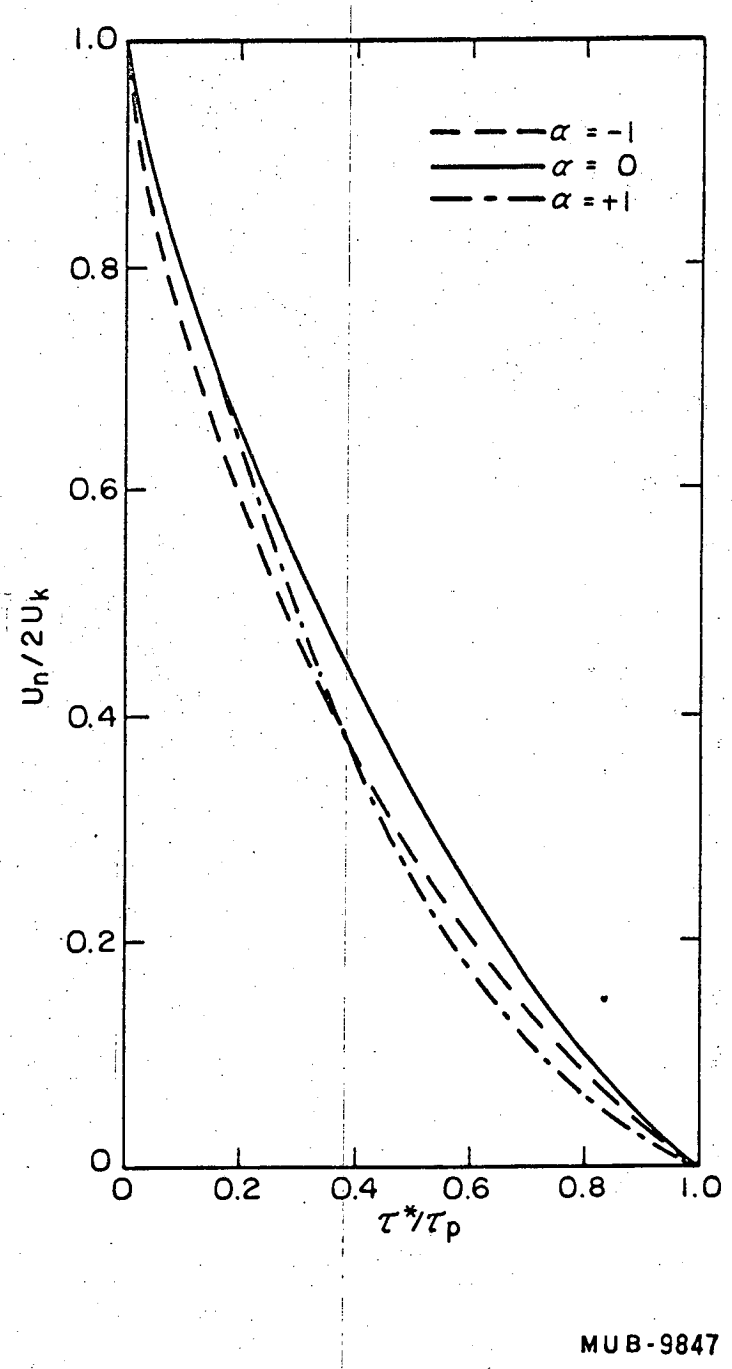

Figure 8. Energy to nucleate a pair of kinks.

$$K = \frac{2\pi U_k}{a\Gamma_o} \Big/ \left(\frac{\tau_p ab}{\pi\Gamma_o}\right)^{1/2} \qquad (6)$$

It is found that the quantity K is only mildly dependent on α, taking on values between 4 and 6 for values of α ranging from +1 to -1. The model also predicts the activation volume $v = -\partial Un/\partial\tau^*$, which is obtained by numerical differentiation of Eq. (5).

It is worthwhile comparing the Dorn-Rajnak model to other recent models on Peierls' controlled deformation due to Seeger[12] and to Friedel[13] who also assume that long range dislocation motion takes place by the thermally activated nucleation of a pair of kinks over Peierls' barriers. In their models, both Seeger and Friedel assume a shape for their critical configurations. Seeger considers the critical configuration to be a pair of half kinks separated by a straight dislocation segment and Friedel takes his kinks to be straight lines joined at a point. Dorn and Rajnak actually calculate the shape of the double kink from minimum energy considerations. Another drawback of the Seeger and Friedel models is their assumption that the dislocation remains in the Peierls' valley even under an applied stress, although this approximation is not too serious in the case of Seeger's model since he only considers the situation in the limit of $\tau^* << \tau_p$. Seeger explicitly includes in this calculation the effect of kink-kink interactions in a form which may not be valid for small kink separations. Friedel and Dorn and Rajnak include the knik-kink interactions indirectly via the line energy. In their model, Dorn and Rajnak have allowed for deviations from a

purely sinusoidal potential and have shown that this only slightly affects the form of Eq. (5). One can argue that the family of functions represented by Eq. (1) is restrictive; however, more recently Dorn and Wallace[14] have recalculated the energy for the case of parabolic potential hills and find once again that the shape of the potential hills is of secondary importance. Although Seeger's model allows for deviations from a sinusoidal potential, his final equations are solved only for the simple case. Friedel restricts his model to the sinusoidal case.

There is little doubt that the calculation of the energy to form a double kink is treated most rigorously and in the greatest detail by the Dorn-Rajnak model; it does not, however, entirely take into account the kink-kink interactions.

The next part of the Dorn-Rajnak model concerns itself with relating the strain rate to the energy Un. Here the usual approximate Boltzmann approach is used with the result that

$$\dot{\gamma} = \rho ab \frac{L}{w} \nu e^{-Un/kT} \qquad (7)$$

where $\dot{\gamma}$ is the shear strain rate, ρ is the dislocation density, L is the average dislocation length swept out by a pair of kinks, w is the critical separation of an embryonic pair of kinks and kT has its usual meaning of the Boltzmann constant and the absolute temperature. In deriving Eq. (7) the simplifying assumption is made that w is independent of the stress; however, the effect that this assumption may have is difficult to evaluate. It is further assumed that even at very low stress all

the pairs of kinks are nucleated in the direction of the applied stress thus giving rise to strain. This is not true in the limit of very small stresses and consequently in that limit one might expect a slight overestimate of the strain rate. However, this model has already been compared with experiment in the cases of Ag_2Al,[15] AgMg,[16] and tantalum,[17] and in all those cases agreement between experiment and theory was found over the whole range of stress including the low stress region in question. In the case of molybdenum[18] a slight deviation from the theoretical line was observed but only in the range below $\tau^*/\tau_p \sim 0.02$.

It is also an implicit assumption of the model that all dislocations are lined up with the Peierls hills and that no macroscopic strain occurs before some double kinks are nucleated over Peierls' barriers. In materials such as iron, electron microscopic studies have not shown dislocations lying parallel to close packed directions. The average randomly oriented dislocation in a slip plane will therefore contain some preexisting kinks which can move at low stresses giving rise to some strain before it is necessary to nucleate new pairs of kinks. Let us briefly examine the maximum magnitude of the strains that could be contributed by such preexisting kinks. Consider a simple Frank network with all dislocations lying in slip planes in a square array. Further consider that the free length of a dislocation is ℓ and the distance between slip planes populated with dislocations is also ℓ. The total length of dislocation line in a unit area of slip plane will then be $2/\ell$ and the dislocation density $\rho = 2/\ell^2$. If we assume that in the extreme case the straightening out of preexisting kinks will cause

the total area of each populated slip plane to be swept out, then the shear strain is simply

$$\gamma = \frac{b}{\ell} = b\left(\frac{\rho}{2}\right)^{1/2}$$

For $b = 10^{-8}$ cm and $\rho = 10^{8}/\text{cm}^2$, $\gamma \approx 10^{-4}$. This implies that the contribution to strain due to sweeping out of preexisting kinks is small, and that taking an offset of $\gamma \approx 10^{-2}$, as was done here, will yield flow stresses related to the nucleation of double kinks. It is interesting to note that in their investigation of the microstrain region in iron, Kossowsky and Brown[19] have identified the low stresses required to move preexisting kinks. Their work is discussed in greater detail below.

Analysis of the Results

The stress which must be applied to cause plastic flow is given by

$$\tau = \tau^* + \tau_A \tag{8}$$

where τ^* is the effective stress discussed above and τ_A is the stress required to overcome the athermal dislocation interactions and will consequently decrease with increase in temperature in the same way as the shear modulus of elasticity.

Recalling the definition of the activaiton volume and using Eq. (7), one obtains

$$v = -\left(\frac{\partial U}{\partial \tau^*}\right)_T = kT\left(\frac{\partial \ell n\dot{\gamma}}{\partial \tau^*}\right)_T \approx kT\left(\frac{\Delta \ell n\dot{\gamma}}{\Delta \tau^*}\right)_T \tag{9}$$

The activation volumes deduced from the data of Fig. 5 by means

of Eq. (9) are plotted in Fig. 9 in terms of the stress τ. Activation volumes for the impure material in three different strain hardened states are also included in the figure. The stress axes were displaced with respect to each other in order to bring all points to a single curve and to correct for the various values of τ_A. The extent of the relative displacement necessary for the points to coincide was found to be closely related to the differences in the flow stresses of the five states at 300°K.

The apparent activation energy U, can be written

$$U = \left[\frac{\partial \ln \dot{\gamma}}{\partial(-\frac{1}{kT})}\right]_\tau \approx \left[\frac{\Delta \ln \dot{\gamma}}{\Delta(-\frac{1}{kT})}\right]_\tau \qquad (10)$$

U was calculated for all five states and plotted against the stress in Fig. 10, with the stress axes displaced as in Fig. 9. Although scatter is apparent the tendencies shown by the three materials are reasonably similar.

The analyses of Figs. 9 and 10 suggest that the Peierls' mechanism is superseded at low stresses (high temperatures) by some other mechanism. In order to compare experiment and theory it is necessary to find a theoretical expression for the dependence of the stress τ^* on the temperature. At high temperatures, thermal fluctuations with energy $2U_k$ become so frequent that plastic deformation takes place even as τ^* approaches zero. The temperature, Tc_1, at which this takes place for a given strain rate, $\dot{\gamma}$, is defined by

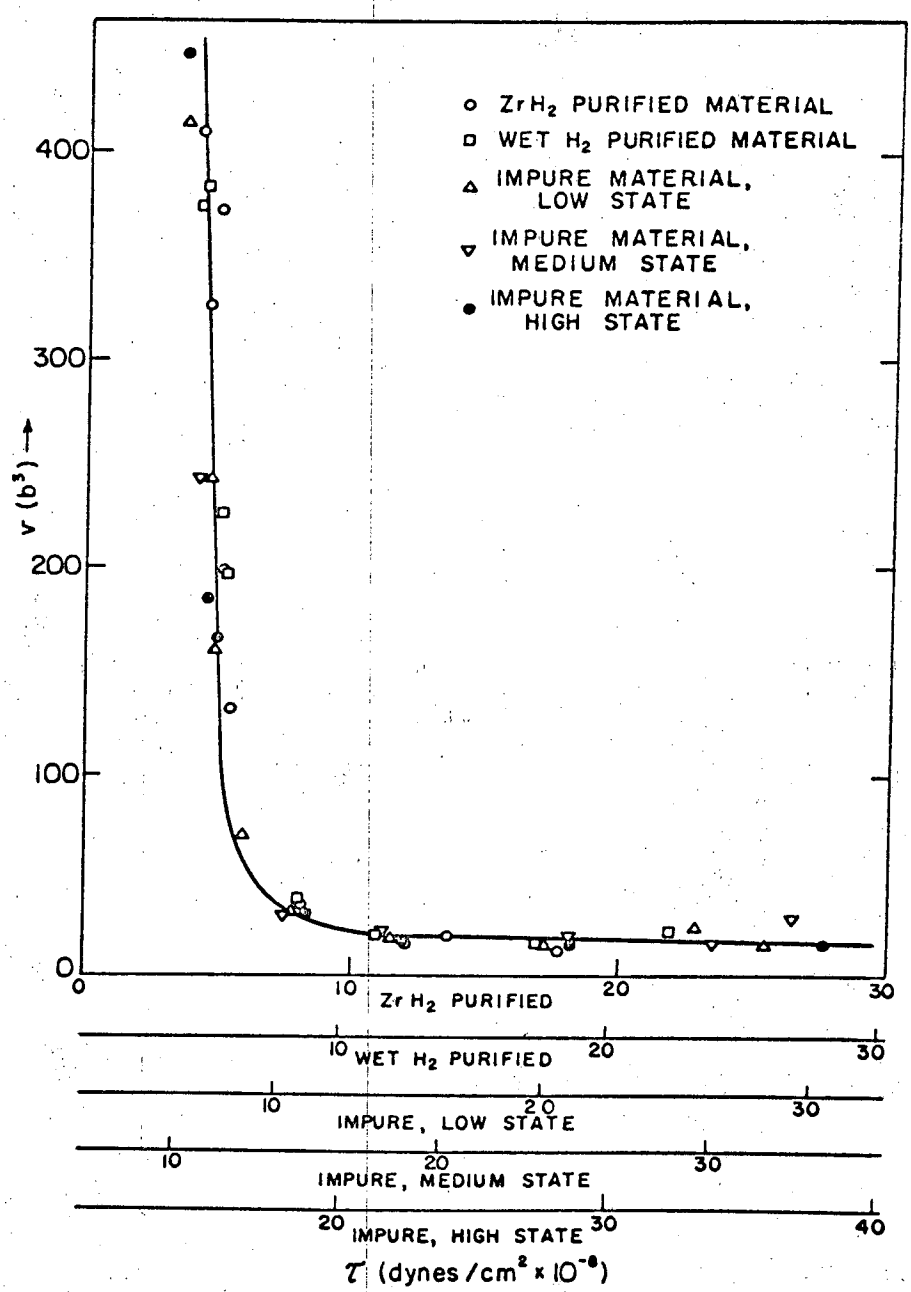

MU-37209

Figure 9. Activation volume vs. stress plot.

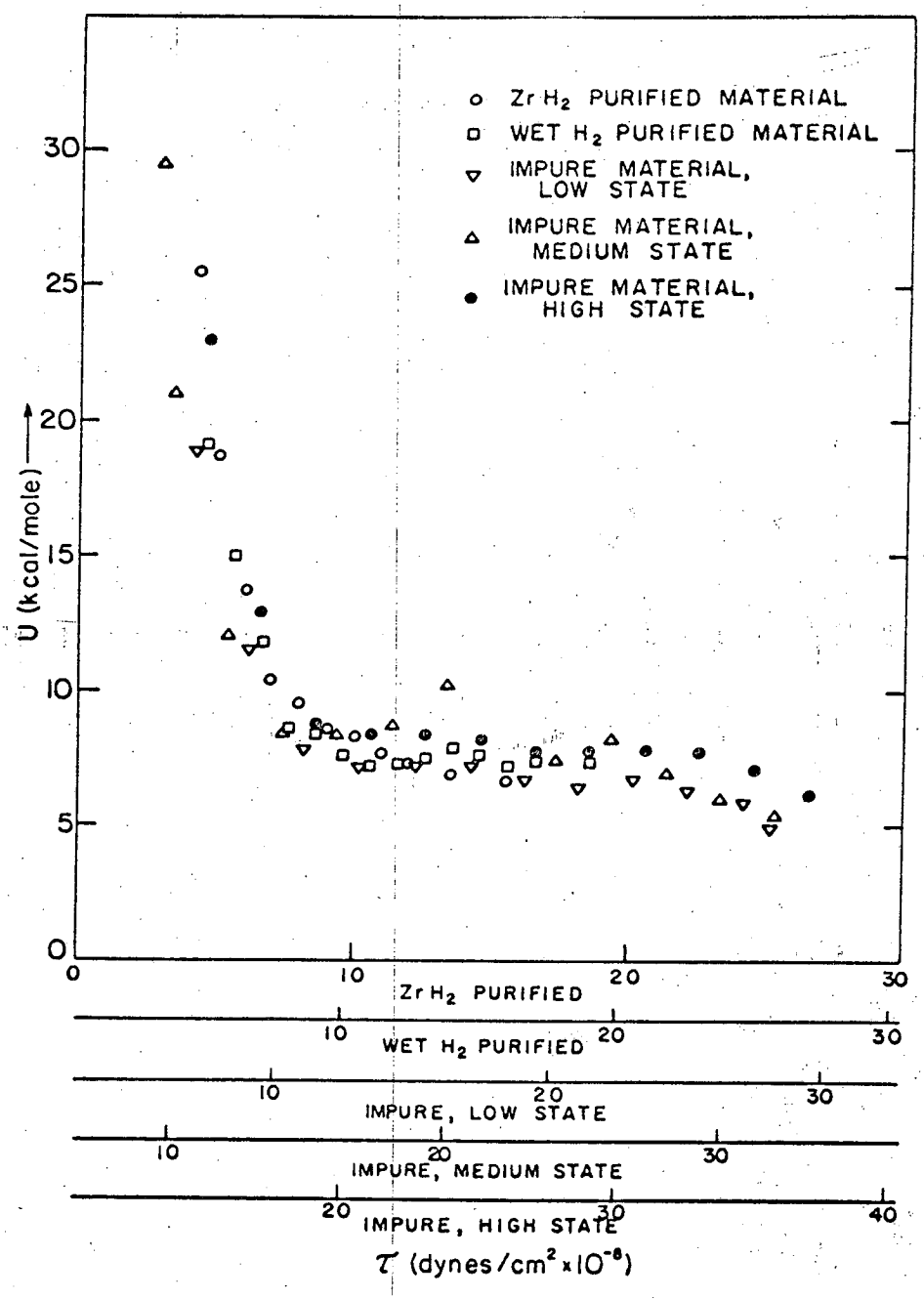

MU-37210

Figure 10. Activation energy vs. stress plot.

$$\dot{\gamma} = \dot{\gamma}_o \, e^{-2U_k/kTc} \tag{11}$$

where we have written $\dot{\gamma}_o = \rho abL\gamma/w$. Comparing Eqs. (11) and (7) we see that

$$\frac{Un}{2U_k} \approx \frac{T}{Tc} \tag{12}$$

or referring to Eq. (5),

$$\frac{\tau^*}{\tau_p} = f_1\left(\frac{Un}{2U_k}\right) \approx f_1\left(\frac{T}{Tc}\right) \tag{13}$$

Both U_k and τ_p change with temperature in the same way as the shear modulus but this effect is small and has been neglected here. The theoretical τ^*/τ_p versus T/Tc curves of Eq. (13) are therefore identical to the relationships given for τ^*/τ_p versus $Un/2U_k$ as shown in Fig. 8. Since τ_p and Tc are not directly available from the data, the data were compared to master plots of the theoretical relationship for different values of τ_p and Tc. All of the data was examined in this way, this included a reanalysis of the data for the impure material which yielded essentially the same parameters as had been determined earlier (c.f. reference 9). The values of τ_p, Tc and τ_A obtained in this way are listed in Table 1. The data points suitably reduced by means of the parameters of Table 1 are given in Fig. 11 where the theoretical curve for the case $\alpha = 0$ is given by the solid line. It can be seen that the upper temperature limit for agreement with the Peierls mechanism has not been significantly affected by the reduction of the interstitial impurity concentration. The values of U_k in Table 1 were obtained from

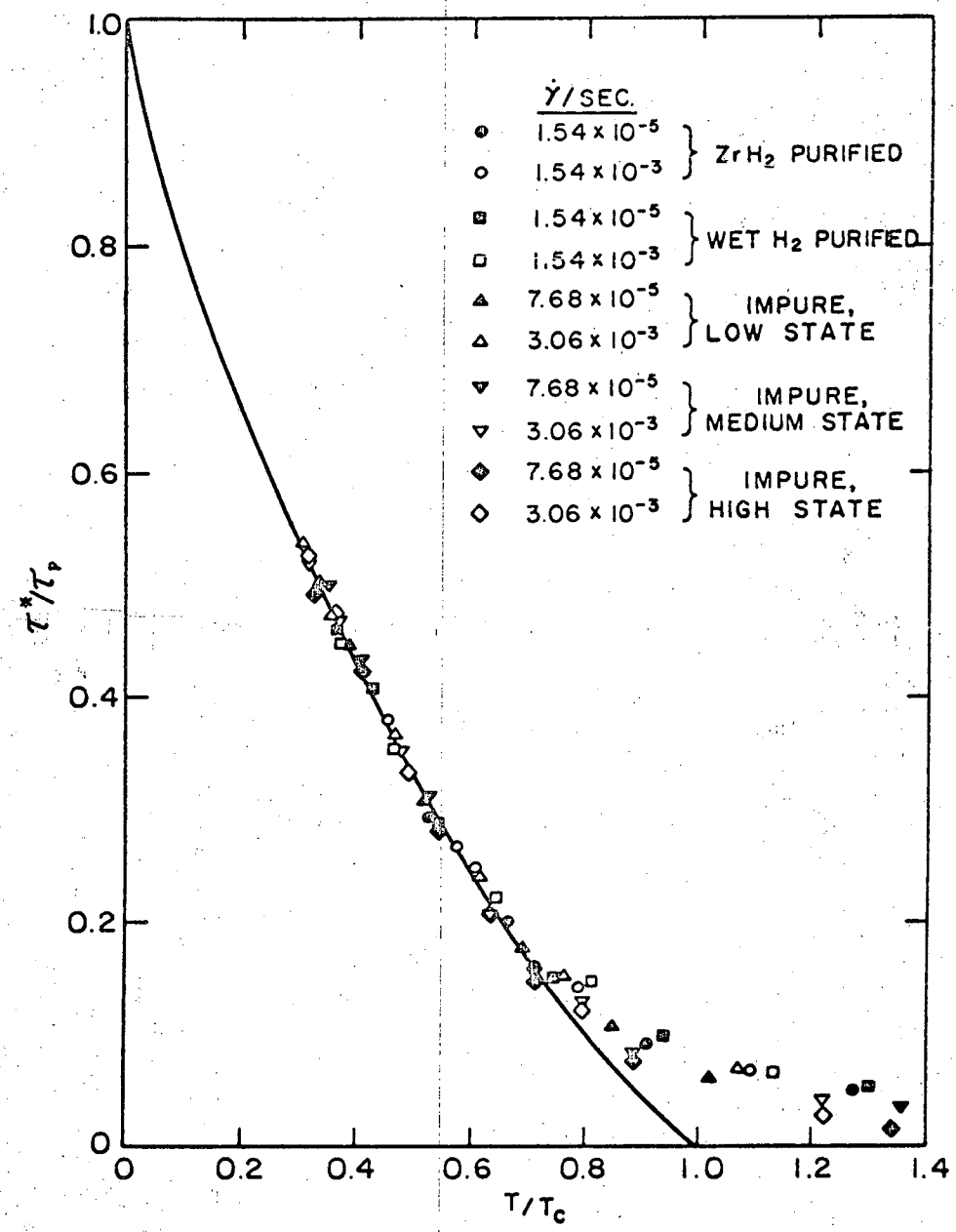

Figure 11. Temperature dependent component of stress vs. temperature, in dimensionless coordinates, comparing data with theoretically predicted curve.

MU-37211

$$\dot{\gamma}_1/\dot{\gamma}_2 = \frac{\exp(-2U_k/kTc_1)}{\exp(-2U_k/kTc_2)} \tag{14}$$

The kink energies obtained in this way from the different purity materials agree fairly well among themselves. The scatter in the values obtained is due to the high sensitivity of Eq. (14) to errors in the determination of the critical temperatures Tc_1 and Tc_2. This same effect is reflected by the scatter in the values of U given in Fig. 10. The line energy is related in terms of the theory to the parameters U_k and τ_p by Eq. (6). For the case $\alpha = 0$, $K = 5.67$. Substituting this value of K into Eq. (6) we can obtain the values of Γ_o listed in Table 1. These values vary between 1.3 and 1.9Gb^2 thus showing reasonable values of the line energy.

Table 1

	τ_p dynes/cm^2 x 10^{-8}	Tc_1 °K	Tc_2 °K	τ_A dynes/cm^2 x 10^{13}	U_k ergs x 10^{13}	Γ_o ergs/cm x 10^4
Impure, high state	47.5	220	245	13.9	5.46	7.53
Impure, medium state	47.5	220	245	9.0	5.46	7.53
Impure, low state	45.0	230	255	4.9	5.98	9.54
Wet H_2 purified	45.0	210	242	3.0	5.07	6.85
ZrH_2 purified	45.0	215	250	2.8	4.93	6.48

In view of the above analysis one can summarize the behavior of iron below about 160°K as follows. At very low temperatures, below 70°K to 100°K depending on purity, twinning appears to be a major mode of deformation as has also been observed by Stein et al.[1] At

temperatures above the twinning range and up to about 160°K the temperature dependence of the flow stress is independent of the strain hardened state and independent of the condentration of interstitial impurities. This suggests an intrinsic lattice resistance to the motion of dislocations. Furthermore, the independence of the activation volume and activation energy on the strain hardened state or impurity content provides additional evidence to the operation of a dislocation mechanism independent of these variables. Finally, the good fit of the data with the theoretical predictions of the Peierls mechanism confirms that this most probably is the rate controlling mechanism of deformation.

It is also possible to show that the other proposed mechanisms described in the introduction are inconsistent with the results reported here.

Stein et al.[1] have proposed that deformation in iron is controlled by the interaction of dislocations with interstitial impurity atoms. They have proposed no quantitative model but regard the decrease in the strong temperature dependence of the flow stress with decrease in interstitial impurity concentration as conclusive evidence for their point of view. In the present work, no such decrease in temperature dependence of the flow stress was observed on purification. The discrepancy between the results of Stein et al. and the present work are further discussed below.

Fleischer[2] has proposed a quantitative model for the interaction of dislocations with tetragonal lattice distortions (whatever the nature of the impurity causing the distortion). Although Fleischer

has not applied his theory to the case of interstitial impurities in body centered cubic metals, it has been suggested that this could be done.[1] The equations of Fleischer however make the flow stress a function of impurity concentration and this has not been observed in this work. The same type of objection applies to the suggestion of Mordike and Haasen that the deformation process is controlled by interactions of dislocations with clusters of impurity atoms.

Schoeck[4] has proposed that deformation in iron may be controlled by jogs on screw dislocations. If this is so one would expect the activation energy for deformation to be close to the activation energy for self diffusion. The activation energies derived experimentally and reported in Table 1 are only about one quarter of the energy for self diffusion thus making this mechanism unlikely.

Schoeck's earlier suggestion[5] that Snoeck type interactions of interstitial impurity atoms with dislocations might account for the large temperature dependence of the flow stress was shown to be incorrect by Schoeck and Seeger.[20] On making a detailed analysis, they concluded that this type of interaction was athermal.

The data for iron above about 160°K could not be interpreted. The results are characterized by both a temperature and a strain rate dependence of the flow stress thus indicating a thermally activated dislocation mechanism. The data derived from the impure material and wet H_2 purified material could not be examined in detail at temperatures above ~400°K because of the superposition of both dynamic and static strain-aging effects. The data for the ZrH_2 purified material, however,

seems to show an athermal region beginning at ~470°K for $\dot{\gamma} = 1.54 \times 10^{-5}$. Throughout the high temperature region, the activation volume increases rapidly with decreasing stress (see Fig. 9) but this characteristic is affected neither by the strain hardened state nor by the purity of the material. The change in activation volume with strain at a particular temperature was determined by a strain rate change experiment at 340°K and is given in Fig. 12. It can be seen that the activation volume remains constant and is unaffected by strain hardening. The evidence is inconsistent with the intersection mechanism and any other known mechanism. The data seem to indicate the operation of dislocation interactions with some intrinsic structural barrier other than the Peierls hills, the barrier being such that the activation volume increases rapidly with a decrease in stress to very high values. It was thought that magnetic domains might provide this kind of intrinsic barrier. In order to test this possibility a simple experiment was carried out. Identical specimens were tested with and without an applied magnetic field large enough to magnetically saturate the specimen (~30 Kilogauss) and hence to introduce essentially a single magnetic domain in each grain of the specimen. The tests were carried at about 240°K where the presence of a magnetic effect should have been most apparent. The application of a magnetic field was found to have no effect on the flow stress or the activation volume. The nature of the intrinsic barrier is yet open to speculation.

Returning to the Peierls controlled temperature region, the results of this investigation are found to be in disagreement with those

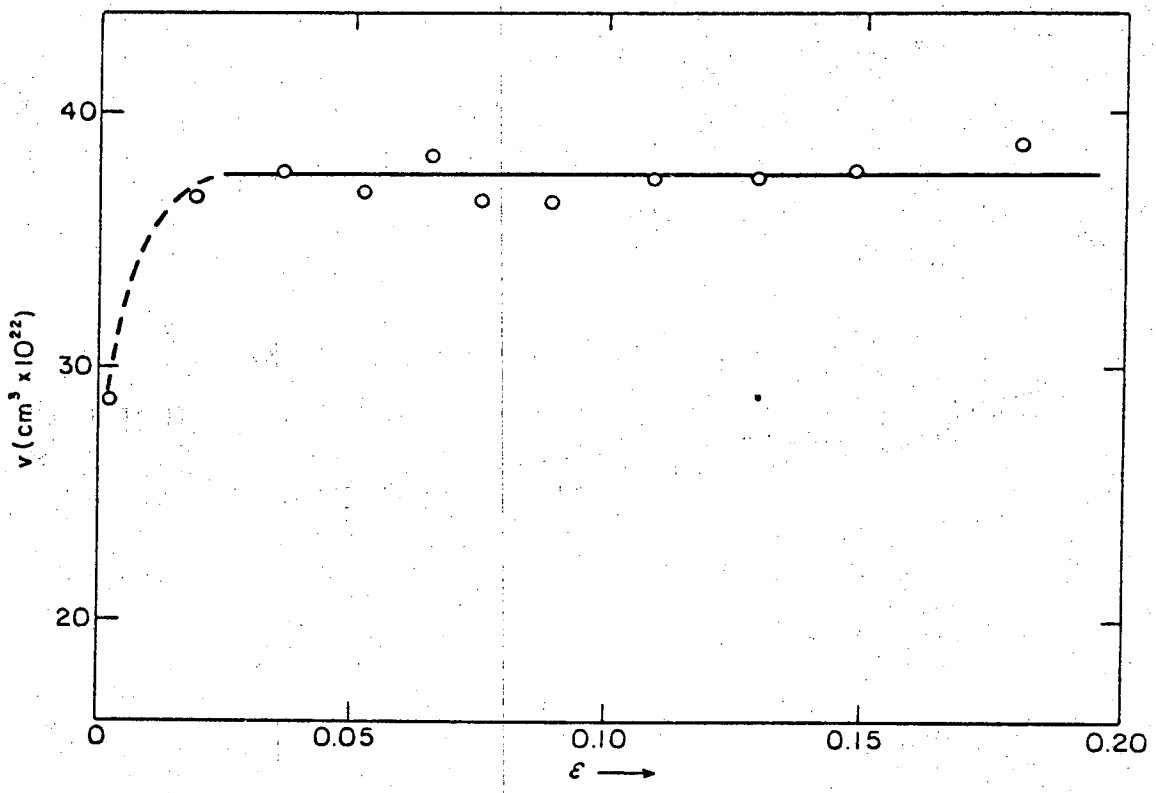

MU-37212

Figure 12. Activation volume vs. engineering strain curve for wet hydrogen purified material at 340°K.

required in the case of cross slip of an undissociated dislocation. Kossowsky and Brown's second stage probably merely represents a transition between straightening out of existing kinks and nucleating new ones.

IV. CONCLUSIONS

The results obtained can be summarized as follows:

(1) The temperature dependence of the flow stress is independent of the strain hardened state or the interstitial impurity concentration.

(2) Below 160°K, the large temperature dependence of the flow stress can be explained on the basis of the Dorn-Rajnak theory of the Peierls mechanism of plastic deformation.

(3) Above 160°K, some other thermally activated intrinsic mechanism seems to be operating.

(4) Removal of interstitials merely decreases the athermal stress level.

V. ACKNOWLEDGMENT

This research was conducted as part of the activities of the Inorganic Materials Research Division of the Lawrence Radiation Laboratory of the University of California. The author wishes to express his appreciation to the United States Atomic Energy Commission for its support of this work. The author is most grateful to Professor John E. Dorn for his guidance and help throughout the course of this research. The author would also like to express his thanks to Dr. Abraham Rosen and Mr. Jack Mitchell for useful discussions of the work.

REFERENCES

1. D. F. Stein, J. R. Low and A. U. Seybolt, Acta Met. (1963) 11, 125.

2. R. L. Fleischer, Phys. Rev. (1962) 33, 3504.

3. B. L. Mordike and P. Haasen, Phil. Mag.(1962) 7, 459.

4. G. Schoeck, Acta Met. (1961) 9, 382.

5. G. Schoeck, Phys. Rev., (1956), 102, 1458.

6. H. Conrad and W. Hayes, Trans. ASM (1963) 56, 125.

7. J. Heslop and N. J. Petch, Phil. Mag. (1956) 1, 866.

8. Z. S. Basinsky and J. W. Christian, Aus. J. Phys.(1960) 13, 299.

9. P. Wynblatt, A. Rosen and J. E. Dorn, Trans. Met. Soc. AIME, (1965) 233, 651.

10. J. E. Dorn and S. Rajnak, Trans. Met. Soc. AIME (1964) 230, 1052.

11. R. Peierls, Proc. Phys. Soc. (London), (1940) 52, 34.

12. A. Seeger, Phil. Mag. (1956) 1, 651.

13. J. Friedel, Dislocations (1964), Pergamon Press.

14. J. E. Dorn and J. Wallace, Private communication.

15. A. Rosen, J. D. Mote and J. E. Dorn, Trans. Met. Soc. AIME, (1964), 230, 1072.

16. A. K. Mukherjee and J. E. Dorn, Trans. Met. Soc. AIME, (1964), 230, 1065.

17. S. Ranji, M.S. Thesis, University of California, Berkeley (1966).

18. S. Lau, M. S. Thesis, University of California, Berkeley (1966).

19. R. Kossowsky and N. Brown, Acta Met. (1966) 14, 131.

20. G. Schoeck and A. Seeger, Acta Met. (1959), 7, 469.

21. A. S. Keh, Private communication.

This report was prepared as an account of Government sponsored work. Neither the United States, nor the Commission, nor any person acting on behalf of the Commission:

A. Makes any warranty or representation, expressed or implied, with respect to the accuracy, completeness, or usefulness of the information contained in this report, or that the use of any information, apparatus, method, or process disclosed in this report may not infringe privately owned rights; or

B. Assumes any liabilities with respect to the use of, or for damages resulting from the use of any information, apparatus, method, or process disclosed in this report.

As used in the above, "person acting on behalf of the Commission" includes any employee or contractor of the Commission, or employee of such contractor, to the extent that such employee or contractor of the Commission, or employee of such contractor prepares, disseminates, or provides access to, any information pursuant to his employment or contract with the Commission, or his employment with such contractor.